Narrow bandgap quantum dot diode structures and photoresistors for thermo-photovoltaic and infrared applications

Karen M. Gambaryan*

Department of Physics of Semiconductors and Microelectronics, Yerevan State University, 0025, Armenia

*Corresponding author

DOI: 10.5185/amlett.2018.1804
www.vbripress.com/aml

Abstract

For the thermophotovoltaic (TPV) and other mid-infrared applications, the narrow bandgap quantum dot (QD) diode structures and photoresistors (PR) based on InAsSbP alloys and InAs industrial substrates are fabricated and investigated. For the nucleation of InAsSbP composition strain-induced QDs in Stranski–Krastanow growth mode, as well as at the growth of emitter epilayer lattice-matched with the InAs(100) substrate, the modified liquid phase epitaxy (MLPE) technique is employed. The HR-SEM and AFM microscopes are used for characterization. The grown QDs surface density equals to $(3\text{-}8)\times10^9$ cm^{-2}, with height and width dimensions ranges from 4 nm to 15 nm and 10 nm to 35 nm, respectively. The current-voltage characteristics and photoresponse spectra of QD TPV and PR structures are also explored. The red shift of the absorption edge, as well as enlargement toward the short wavelength region is revealed for both QD-based devices. The quantitative calculations show increasing of QD-based TPV structures efficiency up to 16% compared with the same structures without QDs.

Keywords: TPV, quantum dots, diode heterostructures, photoresistors, mid-infrared.

Introduction

It is well known that one of the main challenges in the field of renewable energy, in particularly at solar power generation, is to use almost whole spectrum of solar radiation. Traditional industrial photovoltaic (PV) systems mainly convert the visible and near infrared parts of the solar spectrum. Another type of PV systems, which called thermo-photovoltaic (TPV) power generators or TPV cells, convert to electricity the mid-infrared part (2–5 μm wavelengths) of the solar spectrum, as well as the thermal radiation of other heat sources **[1,2]**. From this point of view, TPV cells are used not only in the traditional PV systems, but also for several special applications in mid-infrared region. According to wavelengths region mentioned above, narrow bandgap semiconductor materials with the bandgaps ranging from 0.2 eV to 0.6 ev, have to be used **[3]**. However, as the theoretical calculations show, a maximum efficiency and power density of TPV cells are achieved using semiconductor materials with the band-gaps between 0.2–0.5 eV, which correspond to heat sources temperature within 1200-2500 K. InGaAs ternary and InGaAsSb quaternary alloys grown on InP and GaSb substrate are the traditional material systems for TPV cells **[1-3]**. One of the alternatives to the mentioned above material systems are InAsSbP quaternary solid solutions grown on InAs substrate. Diode structures based on InAsSbP alloys are used not only as TPV cells, but also as photodetectors and light emitting diodes in mid-infrared region.

In contrary to thermoelectric and thermionic converters **[4]**, TPV cells consist of heat source, selective filter and a diode structure, which directly convert heat radiation to electricity. Modern TPV systems can provide efficiency ~20%, with the possibility to reach up to ~40% using cascade multijunction and multispectral semiconductor structures. Relatively small, low weight and not moving constructing parts allow using TPV cells not only in conditions of life and industry, but also in many special applications, such as long-term missions in universe **[4]**, in nuclear reactors, etc.

Last decade it was shown that application of QDs and other nanostructures in semiconductor devices allows to improve their output characteristics **[5,6]**. In particularly, QDs embedded in p-n junction space charge region decrease the threshold current density of semiconductor lasers, provide the red shift in photoresponse spectra and increase the sensitivity and operating temperature of infrared detectors, as well as to increase the fill factor and efficiency of TPV and PV solar cells, etc. All mentioned above advantages are reached due to very interesting and fundamental properties of QDs, where charge carriers (electrons and holes in semiconductors) are localized in all three dimensions.

Because in this paper we describe also our efforts to fabricate the mid-infrared QD photoresistors (PR), which are also called as photoconductive cells, it should be noted that as photon detectors they have many advantages compared with thermal photodetectors, for instance high

photoresponse speed, low cost, etc. Depending on wavelength region they work, corresponding semiconductor materials are utilized. However, as for infrared PRs, especially work in mid- and far-infrared regions, generally, II-VI and III-V narrow bandgap semiconductors and their solid solutions are used. Mid- and far-infrared PRs mainly work at low (cryogenic) temperatures, which is necessary to decrease the dark current and increase photosensitivity. From the other hand, cryogenic engineering system, along with the corresponding optical system lead to increasing PRs weight and cost. Therefore, application of new materials and technologies, development of new approaches based on nowadays physical and engineering principles are very important tasks for the fabrication of modern and high sensitive mid- and far-infrared PRs, especially operate at high (up to room) temperatures.

From this point of view, PRs and photodetectors with QDs or other nanostructures **[7,8]**, where sub-bandgap transitions occur, allow to partially solve mentioned above problems. Theoretical calculation and experimental results show that nanostructures based PRs and photodetectors can operate at up to room temperatures with light loss in sensitivity. Their dark current is also much lower than that of devises without QDs. Additionally note, that all mentioned above semiconductor devices with nanostructures are very important for not only the renewable energy and other special applications, but also can be successfully used in chemistry, biology, medicine, etc.

In this report, we describe the growth and investigation of the n-InAs/p-InAsSbP diode heterostructures and the InAs-based infrared PRs with QDs for TPV and other mid-infrared applications.

Experimental

Stranski–Krastanow (S-K) growth mode **[9]** is one of the most useful approach at the growth of self-organized and dislocation-free QDs and other nanostructures. InAs, InP and InSb III-V compound semiconductors have sufficiently large difference in the diameters of the V element, which allows to provide and monitor QDs nucleation conditions at the S-K growth mode. InAsSbP solid solution is a promising candidate because it can cover the 2–5 μm mid-infrared region. Actually, we have shown **[5-7]** that MLPE technique can be successfully used for the growth of InAsSbP QDs together with MBE and MOCVD techniques traditionally used at the growth of nanostructures.

The samples under consideration (QDs, epitaxial layers and diode heterostructures) were grown by MLPE using a slide-boat crucible. As at traditional LPE process, in this case the nucleation of QDs and the growth of epilayers were performed at closer to thermodynamically equilibrium technological conditions. Purified by the palladium filters hydrogen was used as an ambient gas. The industrial undoped InAs(100) substrates with the diameter of 11 mm and the background impurity concentration of $n=2\times10^{16}$ cm^{-3} were used. To provide the QDs nucleation at the S-K growth mode, undersaturated by arsenic and supersaturated by antimony liquid was used. According to In-As-Sb-P material system phase diagram, in order to provide a lattice mismatch between the substrate and a wetting layer up to 2%, the compositions of InAs, Sb and InP in the liquid phase were chosen as X_{InAs} = 1.95%, X_{Sb} = 12.28% and X_{InP} = 1.7×10^{-2}%, respectively. An undoped InAs and InP crystals, 6N-Sb and a 7N-In were used at preparation of the liquid phase. After long-term homogenization at T=550◦C, the In-As-Sb-P composition liquid phase was contacted with the InAs(100) surface. In order to provoke nucleation, the temperature of the liquid phase was decreased on 1◦C.

Results and discussion

Exploration of the QDs morphology, i.e. their size, shape and the surface density were performed by HR-SEM and AFM microscopes. Each measurement repeated several times to avoid instrumental uncertainty.

Fig. 1 displays the HR-SEM – (*a*) (S=9×9 μm^2) and AFM – (*b*) (S=3.5×3.5 μm^2) images of InAsSbP uncapped QDs grown by MLPE on an InAs(100) substrate.

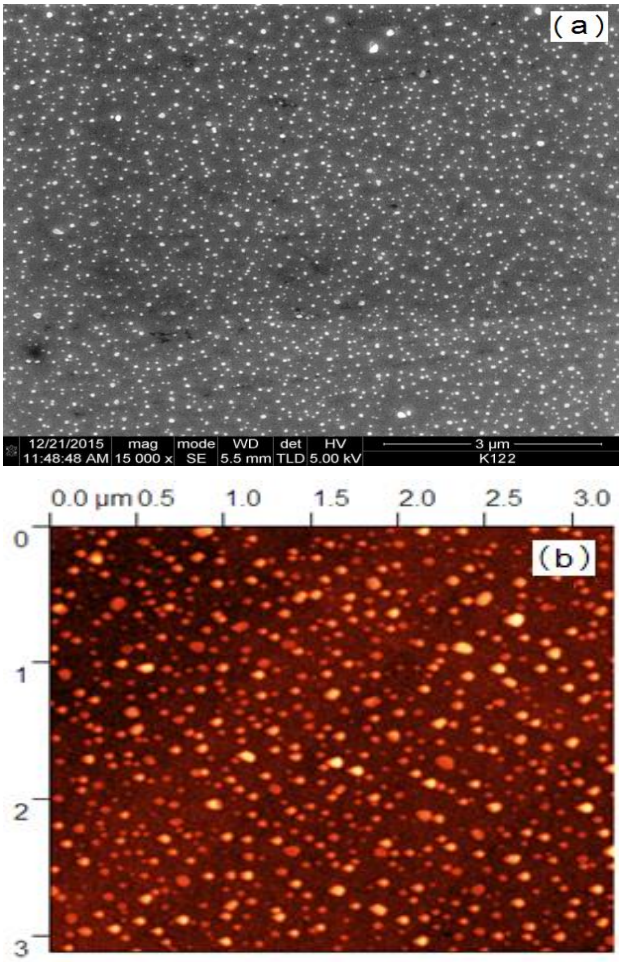

Fig. 1. SEM – (a) and AFM – (b) images of InAsSbP uncapped QDs grown by MLPE on InAs(100) substrate.

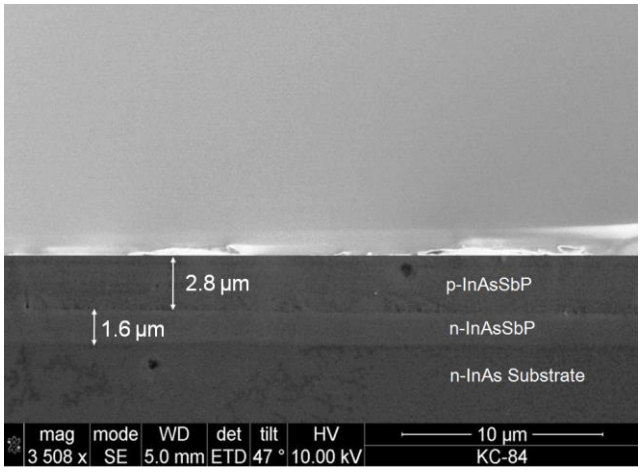

Fig. 2. The HR-SEM image of an n-InAs/n-InAsSbP/p-InAsSbP QD TPV structure's cross-section.

HR-SEM and AFM images show that QDs are uniformly distributed with the surface density of (6–8)×10^9 cm^{-2}. The QDs heights and diameters ranging from 0.5 to 20 nm and from 15 to 70 nm, respectively. The QDs material system and an InAs substrate lattice parameters difference is large enough to provide the growth process in Stranski–Krastanow growth mode [9]. The optimum diameter of QDs equals to ~50 nm was revealed by Gauss fit of the QDs number versus their diameter. Calculation was evaluated from the substrate surface of S=10 μm^2.

The HR-SEM image of the cleavage of n-InAs/QDs/n-InAsSbP/QDs/p-InAsSbP TPV structure is presented in **Fig. 2**.

Transmission electron microscopy (TEM) measurements reveal quantum dots in both substrate-layer and layer-layer interfaces. TEM image of the p-InAsSbP/n-InAs diode heterostructure's cross-sectional area with QDs is presented in **Fig. 3.**

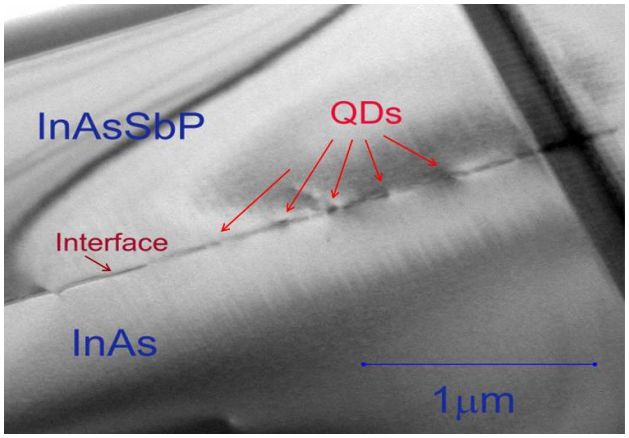

Fig. 3. TEM image of the n-InAs/p-InAsSbP diode heterostructure's cross-sectional area with QDs.

The current-voltage (J–V) characteristic of a diode heterostructure n^+-InAs / n-InAs / QDs / p-InAsSbP was measured at room temperature. The experimental dependence of the dark current I on the voltage V applied to the diode is well described by the following equation.

$$J(V) = J_0\left[\exp\left(\frac{e(V - JR_S)}{nkT}\right) - 1\right] + \frac{V - JR_S}{R_{Sh}}$$

where J_0 – saturation current density, R_S, R_{sh} – series and shunt resistances, respectively, k – Boltzmann's constant, T – absolute temperature, and n – ideality factor. Fitting of the measured I–V curve to the relationship above yields the following values of diode parameters at T = +20°C: R_S = 1.8 Ω; R_{sh} = 2700 Ω and V_c = 0.14 V, where V_c is the contact potential difference of the p–n junction. The ideality factor fitting the experimental data is close to unit, which indicates a diffusion mechanism of current transfer through the p–n junction. Mentioned above data allow to conclude about a good quality of grown heterostructures.

Next, the photoresponse spectra of fabricated PR and TPV structures were measured. The room temperature normalized photoresponse spectra of the n-InAs/InAsSbP-QDs PR at different biases and n-InAs/QDs/p-InAsSbP diode structure are presented in **Fig. 4(a)** and **Fig. 4(b),** respectively.

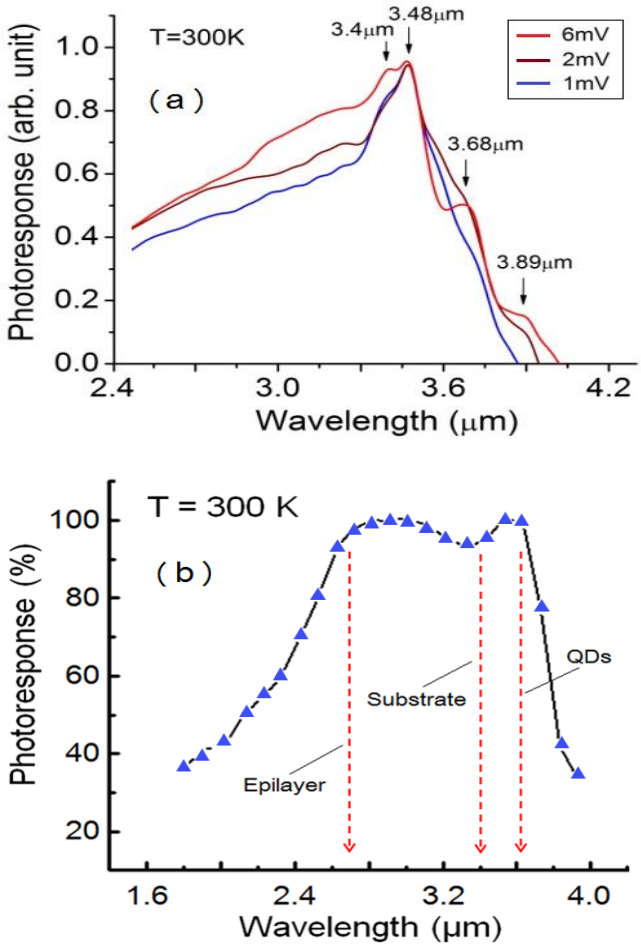

Fig. 4. Normalized photoresponse spectra of the n-InAs/InAsSbP-QDs PR at different biases – (a) and p-InAsSbP/n-InAs diode structure with QDs on the substrate-layer interface – (b).

Photoresponse spectra of fabricated PRs were measured at room temperature applying low biases up to 6 mV. It was found **(Fig. 4a)** that the spectrum is extended up to ~4 μm with the peak at 3.48 μm. This peak coincides with the energy bandgap of InAs (E_g = 0.355 eV). Additional peaks mentioned in figure by arrows are the results of charge carrier's transitions through energy levels created by type-II InAsSbP QDs grown on InAs.

As for TPV diode heterostructure **(see Fig. 4b),** the structure shows photosensitivity in a broad range, which is determined by the sub-bandgap widths of QDs and $InAs_{0.88}Sb_{0.04}P_{0.08}$ quaternary epilayer. The monochromatic radiation responsitivity measured at the maximum of the spectrum was 0.8–1.5 A/W, which corresponds to internal quantum efficiency up to 40% (with allowance for ~30% losses for reflection). Actually, **Fig. 4** shows the red shift of the absorption edges, as well as enlargement of the spectra to the short wavelength region for both QD devices. Our quantitative calculations show increasing of QD-based TPV structures efficiency up to 16% compared with the same structures without QDs.

Conclusion

Thus, the QD n-InAs/p-InAsSbP diode structures and the InAs-based mid-infrared PRs for TPV and other special applications were fabricated and investigated. For the nucleation of InAsSbP composition strain-induced QDs in Stranski–Krastanow growth mode, as well as for the growth of emitter epilayer lattice-matched with the InAs(100) substrate, the MLPE has been used. The QDs morphology and the diode structures' cross-sectional area were characterized by HR-SEM and AFM microscopy. The QDs surface density equals to $(3\text{-}8)\times10^9$ cm^{-2}, with height and width dimensions ranges from 4 nm to 15 nm and 10 nm to 35 nm, respectively. The current-voltage characteristics and photoresponse spectra of both QD TPV and PR structures were also explored. The red shift of the absorption edge, as well as enlargement toward the short wavelength region is revealed for both QD-based devices. The quantitative calculations show increasing of QD-based TPV structures efficiency up to 16% compared with the same structures without QDs.

Acknowledgements

The author wish to thank to the State Committee of Science of Armenia for the financial support (project № 15T-2J137), to Dr. T. Boeck and his colleagues from Leibniz Institute for Crystal Growth (IKZ, Berlin, Germany) for HR-SEM and AFM characterization, as well as to Dr. V. Harutyunyan for photoresponse spectra measurements.

References

1. Wanlass, M.W.; Ward, J.S.; Emary, K.A.; Al-Jassim, M.M.; Jones, K.M.; Couts, T.J.; *Solar Energy Materials and Solar Cells*, **1996**, *41/42*, 405.
DOI: 10.1016/0927-0248(95)00124-7
2. Coutts, T.J.; Ward, J.S.; *Electronic Devices*, **1999**, *46*, 2145.
DOI: 10.1109/16.792010
3. Gevorkyan, V.A.; Aroutiounian, V.M.; Gambaryan, K.M.; Kazaryan, M.S.; Touryan, K.J.; Wanlass, M.W.; *Thin Solid Films*, **2004**, *451/452*, 124.
DOI: 10.1016/S0040-6090(03)01510-4
4. Datas, A.; Martí, A.; *Solar Energy Materials & Solar Cells*, **2017**, *161*, 285.
DOI: 10.1016/j.solmat.2016.12.007
5. Gambaryan, K.M.; *Nanoscale Research Letters*, **2010**, *5*, 587.
DOI: 10.1007/s11671-009-9510-8
6. Gambaryan, K.M.; Aroutiounian, V.M.; Boeck, T.; Schulze, M.; Soukiassian, P.G.; *Journal of Physics D: Applied Physics (FTC)*, **2008**, *41*, 162004.
DOI: 10.1088/0022-3727/41/16/162004
7. Gambaryan, K.M.; Aroutiounian, V.M.; Harutyunyan, V.G.; *Infrared Physics and Technology*, **2011**, *54*, 114.
DOI: 10.1016/j.infrared.2011.01.005
8. Bhattacharya, P.; Su, X.H.; Chakrabarti, S.; Ariyawansa, G.; Perera, A.G.U.; *Applied Physics Letters*, **2005**, *86*, 191106.
DOI: 10.1063/1.1923766
9. Stranski, I.; Krastanow, L.; *Math.-Naturwiss.*, **1938**, *146*, 797.
DOI: 10.1007/BF01798103

